Capillarity

Vol. 16, No. 3, p. 77-86, 2025

Invited review

Capillary-driven processing in carbon fiber-reinforced polymer composites: From multiscale modeling to advanced manufacturing

Zefu Li[1], Yanpei Sun[1], Yonglin Chen[1,2]*, Zhuangjian Liu[3], Yichao Tang[4], Weidong Yang[1,2]*

[1]*School of Aerospace Engineering and Applied Mechanics, Tongji University, Shanghai 200092, P. R. China*
[2]*Shanghai Institute of Aircraft Mechanics and Control, Shanghai 20092, P. R. China*
[3]*Institute of High Performance Computing, A*STAR Research Entities, Singapore 138632, Singapore*
[4]*School of Mechanical Engineering, Tongji University, Shanghai 201804, P. R. China*

Keywords:
Polymeric composites
capillary effect
characterization method
advanced manufacturing

Cited as:
Li, Z., Sun, Y., Chen, Y., Liu, Z., Tang, Y., Yang, W. Capillary-driven processing in carbon fiber-reinforced polymer composites: From multiscale modeling to advanced manufacturing. Capillarity, 2025, 16(3): 77-86.
https://doi.org/10.46690/capi.2025.09.02

Abstract:
The action of capillary pressure plays a crucial role in the formation of voids during the molding process of fiber-reinforced polymer composites. It is primarily driven by surface and interfacial tension, resulting in macroscopic liquid flow controlled by pressure differences. However, due to the influence of microscopic-scale effects, modeling and characterizing the capillary effects in carbon fiber-reinforced polymer composites presents significant challenges. This review offers a comprehensive summary of the relevant theories on capillary pressure, including fundamental theory, average capillary pressure theory, and interface enhancement theory. Furthermore, it discusses methods related to contact angle experiments, capillary pressure experiments, and multiscale numerical simulations while illustrating examples of capillary forces in carbon fiber-reinforced polymer composites. This paper aims to help readers gain a deeper understanding of the mechanisms and applications of the capillary effect in carbon fiber-reinforced polymer composites.

1. Introduction

"Capillarity" refers to the macroscopic movement or flow of liquid influenced by its own surface and interfacial forces (Schwartz, 1969). When the pressure difference or the potential for reducing it through flow disappears, the flow ceases (Liu et al., 2022). The capillary effect frequently arises during composite processing, as reactive liquid monomers or polymers penetrate the initially dry and porous structure created by reinforcing fibers or powders. Composite fabrics or preforms are typically produced in the form of yarns made from reinforcing fibers or filaments with diameters ranging from approximately 7 to 20 μm, exhibiting high anisotropy (Hong et al., 2024). This results in a dual-scale porosity network, with pores ranging from the micron scale between fibers to the millimeter scale between fiber yarns (Michaud, 2021; Li et al., 2023). Influenced by the composite molding process, the capillary effect is often coupled with fluid dynamics, manifested in the externally applied pressure driving the flow, as well as in the coupling with the rheology of the polymer matrix (Zhang et al., 2024; Zhang et al., 2025). Moreover, the viscosity of the polymer matrix in its liquid form is relatively high, resulting in a strong dependence on interface velocity (Wang and Hahn, 2007; Chen et al., 2023b).

Yandy Scientific Press

*Corresponding author.
E-mail address: lizefu@tongji.edu.cn (Z. Li); Pei_Pei@tongji.edu.cn (Y. Sun); chenyonglin@tongji.edu.cn (Y. Chen); liuzj@ihpc.a-star.edu.sg (Z. Liu); tangyichao@tongji.edu.cn (Y. Tang); yangwd@tongji.edu.cn (W. Yang).

Received June 2, 2025; revised June 27, 2025; accepted July 19, 2025; available online July 22, 2025.

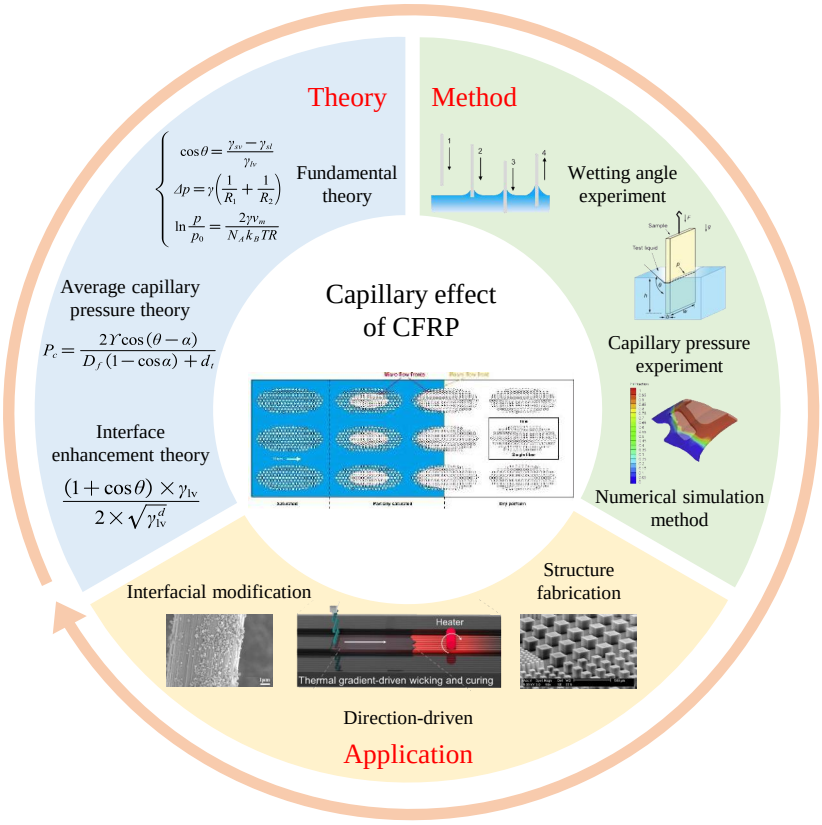

Fig. 1. Schematic diagram of the structure of this review on capillary effects in CFRP.

The study of capillarity in the formation processes of Carbon Fiber-Reinforced Polymer (CFRP) composites presents significant challenges, primarily due to the lack of advanced monitoring technologies capable of capturing the associated temporal and spatial scales of these phenomena (Abry et al., 2001; Behera et al., 2020). The accurate modeling and characterization of capillary effect remains complicated, as it requires precise measurement techniques and robust theoretical frameworks for a comprehensive understanding of the underlying mechanisms (Armstrong et al., 2021; Li et al., 2025). This review provides a deep insight into the critical capillary pressure theories, characterization and simulation methods, and applications relevant to CFRP (Fig. 1). In Section 2, the capillary pressure theories focusing on three key areas are discussed: Fundamental theory, average capillary pressure theory, and interface enhancement theory. Section 3 summarizes the state-of-the-art characterization techniques, including contact angle experiments and capillary pressure experiments. Section 4 introduces the numerical modeling approaches related to capillarity in CFRP, followed by a discussion of capillary applications in CFRP. Finally, the paper is summarized and the future outlook in this field is set forth.

2. Capillary pressure theory

2.1 Fundamental theory

Capillary action refers to the movement of a fluid along a surface without any external force (Deng et al., 2024). Under the basic assumption of neglecting the thickness and structure of the surface and the solid-liquid interface layers, the three fundamental equations of classical capillary theory can be derived. First, Young's equation (Young, 1805) for the contact angle describes the boundary conditions of the wetting phenomenon, which is given by:

$$\cos\theta = \frac{\gamma_{sv} - \gamma_{sl}}{\gamma_{lv}} \tag{1}$$

where γ represents the surface tension; the subscripts sv, sl, lv denote solid-vapor interphase, solid-liquid interphase, and liquid-vapor interface, respectively; θ denotes the contact angle, with 90° as the boundary. When $\theta > 90°$, the surface is considered non-wetting; when $\theta > 135°$, it is classified as superhydrophobic, while if $\theta < 90°$, it is considered wetting. A contact angle of or the absence of a stable contact angle indicates complete spreading. The capillary pressure, that is, the pressure difference between a liquid-gas or liquid-liquid interface, is influenced by the curvature of that interface. Second, Laplace's equation for the excess pressure resulting from interface curvature expresses the connection between this pressure difference and the surface tension:

$$\Delta p = \gamma\left(\frac{1}{R_1} + \frac{1}{R_2}\right) \tag{2}$$

where R_1, R_2 denote the two principal radii of curvature of the surface; γ is the surface tension of the liquid. For a spherical droplet of radius R, the Laplace relation yields $\Delta p = 2\gamma/R$, while for a cylindrical interface of radius R, $\Delta p = \gamma/R$. Third, the change in vapor pressure of a liquid inside droplets or

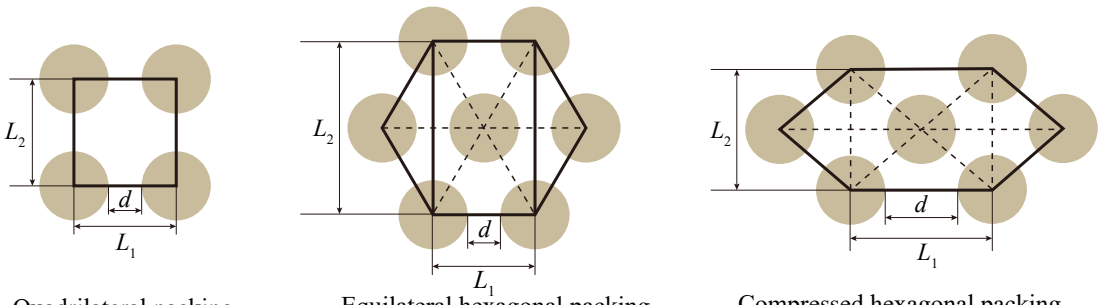

Fig. 2. Fiber structures in tows.

pores due to differences in curvature can be explained by the Kelvin equation (Thomson, 1872), which describes the vapor pressure over curved surfaces. According to the laws of thermodynamics, the saturation vapor pressure p on a curved surface of a pure liquid is determined by the temperature T and the radius of curvature R:

$$\ln \frac{p}{p_0} = \frac{2\gamma v_m}{N_A k_B T R} \tag{3}$$

where the radius of curvature R is positive for convex liquid surfaces and negative for concave liquid surfaces; p represents the saturated vapor pressure on the curved surface; p_0 represents the saturation vapor pressures over a flat liquid surface; v_m denotes the molar volume of the liquid; N_A represents Avogadro's number; and k_B is Boltzmann's constant. The above three equations are collectively referred to as the fundamental equations of classical capillarity.

2.2 Average capillary pressure theory

For a vapor-solid interface, the capillary pressure in a capillary tube refers to the pressure difference caused by surface tension. This can be described by Young's equation, which links the interfacial forces acting on the solid surface, surface tension and contact angle (Duprat et al., 2012):

$$P_c = \frac{2\gamma \cos\theta}{r} \tag{4}$$

where P_c denotes the capillary pressure and r denotes the tube radius. Capillary-driven flow can be defined by the Lucas-Washburn equation (Washburn, 1921):

$$H = \sqrt{\frac{r\gamma \cos\theta}{2\mu} t} \tag{5}$$

where H represents the distance travelled by the liquid front, while t refers to the flow time, and μ is the viscosity of the liquid. The change in mass over time can be expressed as follows:

$$m = \sqrt{\frac{\pi^2 r^5 \rho \gamma \cos\theta}{2\mu} t} \tag{6}$$

where ρ denotes the density of the liquid and m is the mass of the liquid.

As for CFRP, average capillary pressure models have been developed to describe flow within fiber bundles, typically under the assumption of an ideal fiber arrangement (Uematsu et al., 2013). According to scanning electron microscope observations of the fiber tow, typical fiber packing structures can be classified into three types: quadrilateral, compressed hexagonal, and equilateral hexagonal arrangements (Fig. 2). Bayramli and Powell (1990) investigated the influence of the unique structure of fiber bundles by assuming a tetragonal (square) packing arrangement of fibers. In their model, the variations in capillary pressure were characterized as a function of the directional solid angle. Ahn et al. (1991) proposed an analytical expression for capillary pressure on the basis of the volume fraction ratio of fiber bundles, taking into account the effect of bundle structure. Yeager et al. (2016) developed a capillary pressure model that considers the interactions between neighboring fibers in tightly packed tows, where compressed hexagonal packing is used as the representative unit cell (Table 1).

2.3 Interface enhancement theory

In composite materials, the interface serves as a transitional region between the fibers and the polymer matrix (Li et al., 2024), and the quality of this interface has a direct impact on the overall mechanical and physical properties of the composite. In the context of capillarity in composites, the interface enhancement theory typically refers to the use of capillary mechanisms to improve the overall performance of the material. The interaction between fibers and polymer not only influences the capillary-driven liquid infiltration behavior but also determines the adhesion force and bonding strength between them. To enhance the interfacial performance of CFRP, it is necessary to develop relevant interface toughening theoretical models to quantify the extent of these effects (Chen et al., 2023a). Wang et al. (2014) investigated the issue of interface enhancement in hierarchical composites made of Carbon Nanotubes (CNT) and Carbon Fiber (CF). Through droplet tests and analytical models, they developed a theory that incorporates both the grafting force between CNT and CF, as well as the wettability of the CF surface. This theory provides a solution to the problem of balancing CNT grafting density and CF surface wettability to improve the interfacial shear strength of the composite material. Dresel and Teipel (2016) addressed the wetting issue of carbon nanotubes by proposing a theory based on liquid infiltration methods and the Owens, Wendt, Rabel and Kaelble model. It calculates

Table 1. Average capillary pressure model for fiber bundles.

Reference	Theoretical model	Fiber packing
Bayramli and Powell (1990)	$P_c = \frac{2\gamma\cos(\theta-\alpha)}{D_f(1-\cos\alpha)+d_t}$	Hexagonal
Ahn et al. (1991)	$P_c = \frac{F}{D_f}\cdot\frac{V_f}{1-V_f}\gamma\cos\theta$	Quadrilateral
Neacsu et al. (2006)	$P_c = \frac{2\gamma}{D_f}\cdot\frac{\sin(\alpha_{sup}+\theta)-\sin(\alpha_{inf}+\theta)}{\frac{5\pi}{6}\left(1+\frac{d_t}{r_f}\right)-1-\frac{\sqrt{3}}{2}}$	Hexagonal
Yeager et al. (2016)	$P_c = \frac{1}{S_{\max}-S_{\min}}\sum_{1}^{n-1}\frac{1}{2}(P_{c,i}+P_{c,i+1})\Delta s$	Compressed hexagonal

Notes: F represents the form factor; D_f represents the fiber diameter; V_f represents the fiber volume fraction; d_t represents half of the gap between two fibers; α denotes the directional angle; s refers to the fiber surface area wetted. The number of data points in P_c versus dataset is represented by n. denotes the permissible surface area wetted, and the subscripts max, min represent the limits. α_{sup} and α_{int} are the specific values of limits, where $\alpha_{sup} \approx \pi/2-\theta$ and s.

the surface energy of carbon nanotubes and their dispersion and polarity fractions through contact angle measurements, providing a solution for improving the dispersion of carbon nanotubes and selecting appropriate dispersing media based on surface energy. Zhang et al. (2017) presented a theory that combines the modified Wilhelmy method, integrating an enhanced version of the Cassie-Baxter model. This theory addresses the accurate characterization of the wettability of CNT fibers and predicts their physical adhesion to the polymer matrix.

3. Characterization and simulation methods

3.1 Contact angle experiment

Capillary force is strongly influenced by the contact angle (wetting angle), as both are determined by surface tension and the interactions occurring at the liquid-solid interface. The wettability of solid surfaces is commonly characterized by the contact angle formed between a liquid and the solid surface, a property directly influenced by capillary forces arising from surface tension and interfacial interactions. Contact angles are typically measured using either direct optical methods or indirect mechanical approaches. The former (Yuan and Lee, 2013) involve measuring the tangent angle at the three-phase contact point of a liquid droplet. This technique is straightforward and convenient, requiring only a few square centimeters of solid surface area and a few microliters of liquid, making it suitable for small-scale testing. However, the minimal sample quantities increase the risk of contamination, which may compromise the accuracy of contact angle measurements. Additionally, factors such as the identification of droplet profile, the selection of baseline, and the determination of tangent angle introduce subjectivity that can affect the reliability of the results.

In contrast, the Wilhelmy balance method (Yuan and Lee, 2013), an indirect mechanical technique, determines the contact angle by measuring the force exerted on a solid sample (e.g., a thin plate, rod, or fiber) as it interacts with the test liquid. The force detected by the sensor represents a combination of buoyancy and wetting tension and is directly related to capillary forces acting along the liquid-solid interface. If the surface tension of the liquid and the wetted perimeter of the solid are known, the contact angle can be calculated indirectly. This method reduces human subjectivity and improves measurement accuracy through force-based inference. However, for dynamic contact angle measurements, it requires a constant wetted perimeter along the immersion direction and demands high precision in measuring the wetted length of the solid sample.

3.2 Capillary pressure experiment

Capillary pressure can be quantified through wicking experiments, providing a direct and quantitative way of analysis using a single test. These experiments offer initial insights into the capillary pressure characteristics of fiber-reinforced materials, allowing for the assessment of variations in fiber surface properties, volume fraction or pore structure. Amico and Lekakou (2002) introduced a technique where fiber bundles or single-layer fiber-reinforced fabrics are partially submerged in a probe liquid, and the capillary pressure is determined by measuring the rate of weight gain or the height of the liquid rise. Pucci et al. (2015) adopted a Washburn-based measurement approach, in which capillary pressure is evaluated by varying the fiber preform orientation. They successfully determined three advancing contact angles for the weft, warp and through-thickness directions, which were subsequently used to calculate the equivalent capillary pressure. Capillary force measurement methods provide a complementary approach to studying wettability and contact angles, as they directly quantify the forces resulting from liquid-solid interactions. Other techniques such as the capillary rise method measure the height of a liquid column in a capillary tube, which is governed by the balance between capillary forces and gravity. This approach is particularly effective for determining the contact angle and surface tension in liquid-solid systems, as the rise height is related to the contact angle through the Young-Laplace equation. Similarly, the Wilhelmy plate method, in addition to its application for contact angle measurement, can

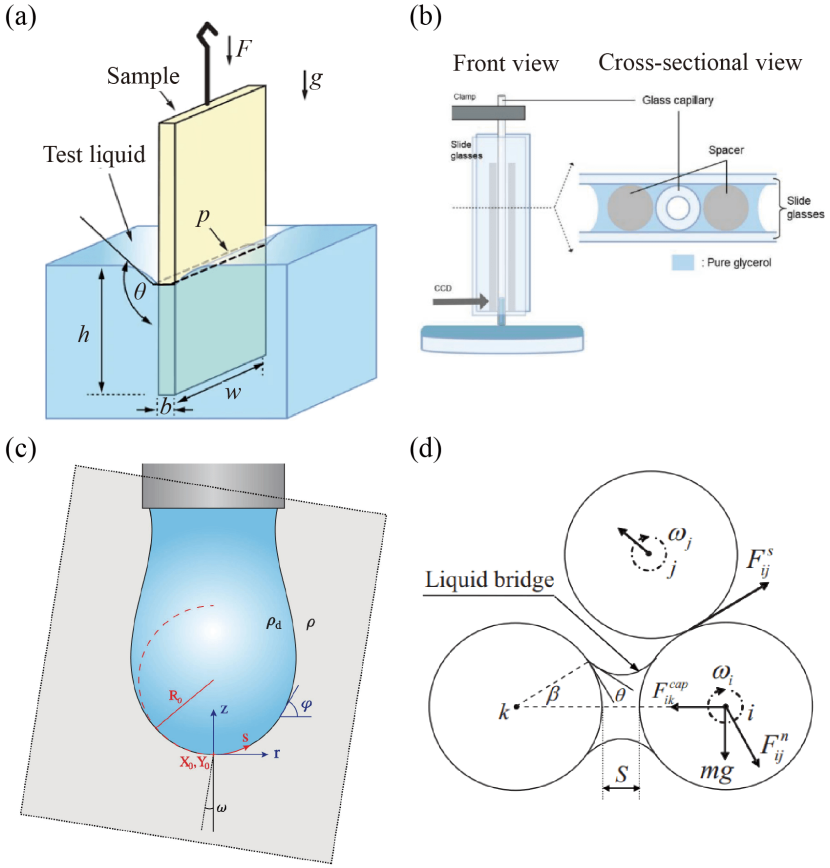

Fig. 3. Schematic of interfacial tension measurements by the (a) Wilhelmy plate method (Daniel et al., 2023), (b) capillary rise method (Kim et al., 2020), (c) pendant drop method (Berry et al., 2015) and (d) rotating drop method (Liu et al., 2011).

be adapted to measure capillary forces by analyzing the force exerted on a partially immersed plate. These forces are closely related to the surface tension of liquid and the cosine of the contact angle, forming a robust relationship between capillary behavior and wettability. Other methods, such as the pendant drop and rotating drop techniques, are primarily employed for measuring interfacial tension, but they can also inform capillary force studies by providing precise surface tension values critical for force calculations. The schematic of the interfacial tension measurement setup and the capillary force measurement configurations are presented in Fig. 3.

The experimental principle of the Wilhelmy plate technique (Daniel et al., 2023) is as follows: A flat plate with a known surface area is vertically immersed in a liquid, causing it to adhere to the plate surface. The adhesive force is continuously monitored using a force sensor. Subsequently, the interfacial tension (γ) is calculated using the measured force (F), the perimeter of the plate (L), and the liquid contact angle (θ):

$$\gamma = \frac{F}{L\cos\theta} \tag{7}$$

The experimental principle of the capillary rise method (Kim et al., 2020) is as follows: A capillary tube is directly immersed in a liquid, and the liquid rises along the tube wall due to capillary forces until equilibrium is reached. Through mechanical analysis, the force balance condition at the liquid surface can be directly obtained, allowing the corresponding interfacial tension to be calculated:

$$\gamma = \frac{1}{2}(\rho - \rho_g) g h r_0 \cos\theta \tag{8}$$

where r_0 represents the radius of the capillary tube, h indicates the height of the liquid column, and g is the product of the density and gravitational acceleration of the liquid.

The experimental principle of the pendant drop method (Berry et al., 2015) involves suspending a droplet in a different phase and measuring the surface tension by observing the droplet shape:

$$\frac{-\frac{\mathrm{d}^2 r}{\mathrm{d}z^2} + \frac{1}{r}\left[1 + \left(\frac{\mathrm{d}r}{\mathrm{d}z}\right)^2\right]}{\left[1 + \left(\frac{\mathrm{d}r}{\mathrm{d}z}\right)^2\right]^{\frac{3}{2}}} = \frac{p_0 - \Delta\rho\, g z}{\gamma} \tag{9}$$

where r represents the radial position or the radius of the droplet along the vertical (axial) direction, z is the height measured from the apex of the droplet, p_0 is the pressure at the point of suspension, Δp denotes the density difference between the two phases, and g is the gravitational acceleration.

The experimental principle of the rotating drop method (Liu et al., 2011) involves considering the effects of centrifugal force, gravity and interfacial tension on the shape of the liquid

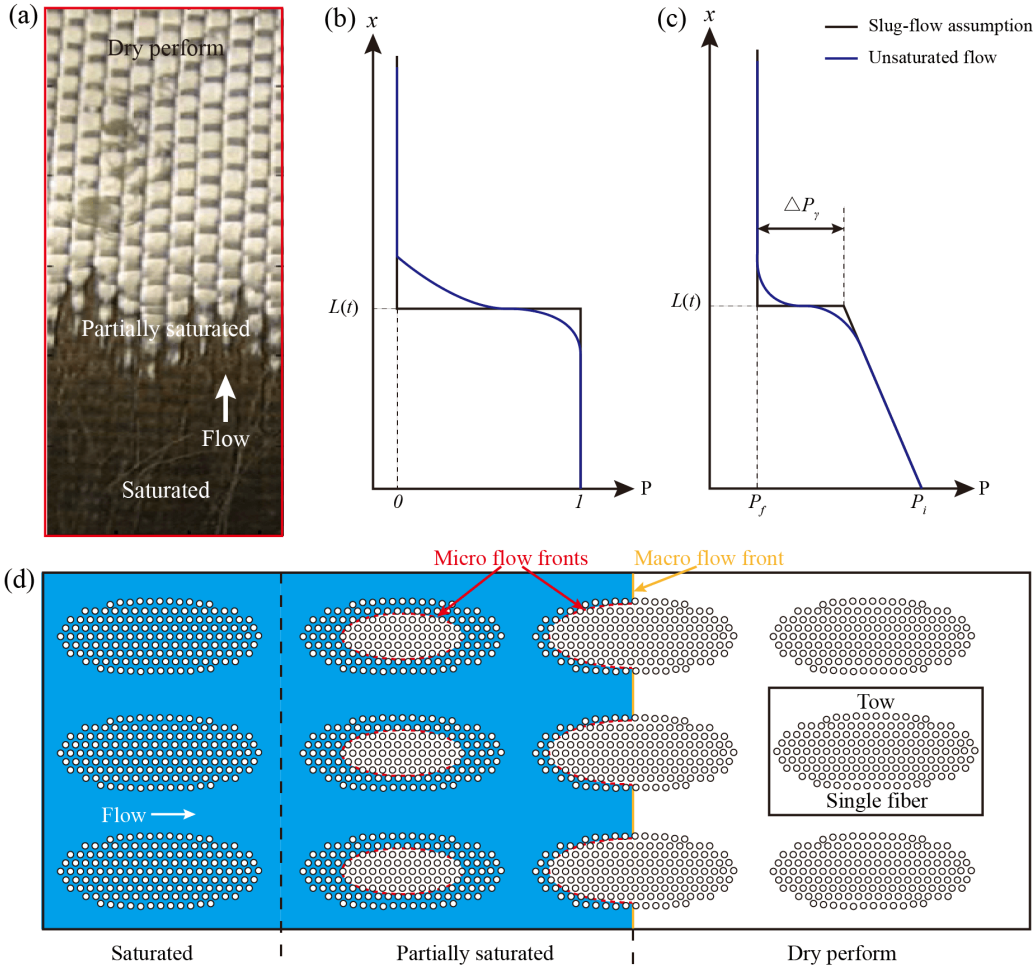

Fig. 4. Micro flow and macro flow: (a) Resin infiltrating flow (Nordlund and Michaud, 2012), (b) saturation, (c) capillary pressure and (d) schematic representation of micro flow and macro flow.

during rotation, in order to measure the interfacial tension:

$$\gamma = \frac{\Delta\rho\omega^2 D^3}{4} \tag{10}$$

where ω denotes the angular velocity, D represents the diameter of the droplet's short axis, and L refers to the length of the droplet's long axis.

3.3 Numerical simulation method

Capillary action in CFRP is jointly governed by the complex microstructure–such as fiber arrangement, nanoparticle distribution and pore network–and the wetting properties at the liquid-solid interface (Cai et al., 2022; Zhou et al., 2023). Experimental characterization methods, including direct measurements of contact angle and capillary pressure, provide critical data for quantifying wettability. However, these methods face limitations in capturing nanoscale interfacial effects and dynamic infiltration behavior within complex porous structures (Cai et al., 2021; Zhou et al., 2024). Numerical simulations, via constructing multiscale mathematical models that integrate surface tension, contact angle and fluid mechanics principles, can predict liquid infiltration paths and capillary force distributions within fiber bundles, pores and nanoparticle networks, thus compensating for the limitations of experimental techniques (Teixidó et al., 2022). Capillary effects primarily manifest at the microscale, while macroscopic observations are generally regarded as the result of microscale phenomena occurring within fiber tows (Liu et al., 2024). It is commonly understood that as the infiltrating liquid gradually saturates the fiber preforms, a nonlinear pressure distribution occurs within the unsaturated areas (Fig. 4). In partially saturated regions, the pore size has a significant impact, causing capillary forces to act over a broader length scale. Therefore, at the macroscopic level, the magnitude of capillary pressure is typically represented by the average capillary force of the representative volume elements at the microscopic scale. Chang et al. (1997) classified resin flow into two flow regimes: macroflow around the fiber bundles and microflow around individual fibers within the bundles, which occur simultaneously and are both governed by Darcy's law. A detailed numerical simulation of capillary effects under low flow velocities during the resin transfer molding process was conducted using a body-fitted finite element method, which accounts for the complex geometry of the fiber preform. Lawrence et al. (2009) conducted numerical simulations of capillary effects via a multiscale modeling approach using the

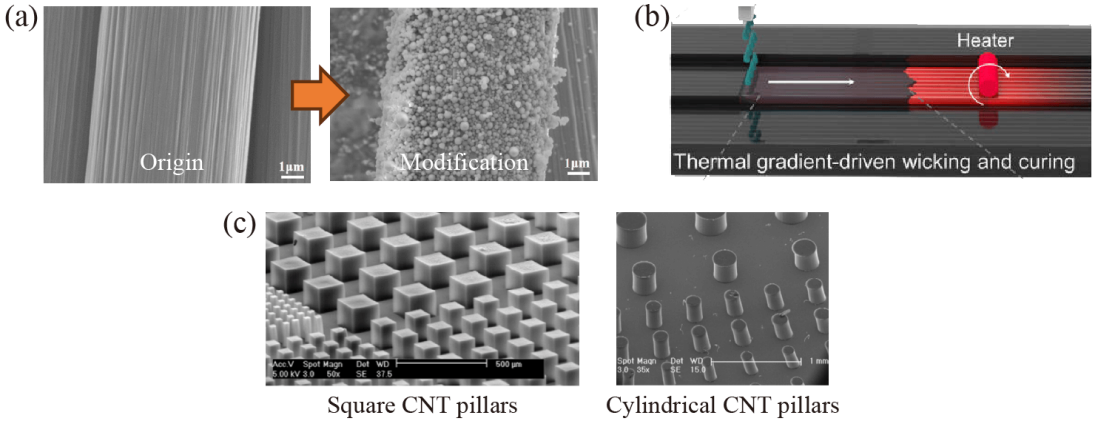

Fig. 5. Application of capillary force in CFRP: (a) Interfacial modification (Yao et al., 2021), (b) direction-driven approach (Shi et al., 2020) and (c) structure fabrication (García et al., 2007).

liquid injection molding simulation software. By introducing capillary pressure at the fiber bundle level, they modified the existing simulation tools to enable the prediction of the saturation process within the bundles. Capillary pressure was incorporated as an additional force in the boundary conditions of the fiber bundles, and the capillary effect was simulated by varying the pressure at the vent locations.

In the numerical simulation of capillary-driven resin infiltration in CFRP, the material is typically modeled as a porous medium (Chen et al., 2023b). Porous media models effectively describe both macroscopic and microscopic flow using Darcy's law and the Young–Laplace equation. These models simplify complex geometries, reduce computational cost and facilitate the integration of capillary pressure and wettability parameters. Compared to the direct simulation of individual fibers or pores, porous media models offer significant advantages in terms of computational efficiency and compatibility with experimental data. Using a multiscale modeling technique, Park et al. (2011) conducted numerical simulations to investigate the impact of capillary effects on void formation and the saturation of fiber bundles. By comprehensively considering the flow characteristics within macropores (between fiber bundles) and micropores (inside the bundles), they proposed a model to describe void formation and saturation behavior induced by capillary action during the manufacturing of fiber-reinforced composites. Viscous flow between fiber bundles was modeled using Darcy's law, while the influence of capillary pressure on intra-bundle flow was explicitly incorporated. Via evaluating the timescales of resin infiltration across different pore domains, the authors predicted the tendency for void formation and analyzed the impact of capillary effects on fiber bundle saturation. Devalve and Pitchumani (2013) performed numerical simulations of capillary effects using a volume of fluid-based method coupled with the momentum equation. They explored capillary-driven resin infiltration in plain weave fabric preforms and considered the influence of key parameters–such as fiber bundle geometry, fiber volume fraction, fiber diameter, resin surface tension, and contact angle–on capillary pressure. The flow behavior of resin within the fiber bundles was simulated by integrating porous media and capillary source terms into the momentum equation, and the results demonstrated that capillary action has a significant influence on void formation and distribution. Furthermore, a parametric study was conducted to examine the effects of the capillary number and Reynolds number on void content and distribution: Andriamananjara et al. (2019) carried out an in-depth study of capillary effects during resin infiltration in plain weave fabric preforms. Their model incorporated the influence of key parameters–such as fiber bundle geometry, fiber volume fraction, fiber diameter, resin surface tension, and contact angle–on capillary pressure. By introducing porous media source terms and capillary source terms into the momentum equation, they could simulate the resin flow behavior within the fiber bundles.

4. Applications

The application of capillary forces in interfacial modification of composites utilizes the capillary behavior of liquids within micropores or fibrous networks to precisely tailor the interfacial properties (Fig. 5). Tawfick et al. (2013) revealed the densification mechanism of CNT microstructures during the liquid evaporation process using a capillary-driven assembly technique. Their study demonstrated that the anisotropic mechanical properties of the CNT forest and the frictional interactions between the CNTs significantly influence the capillary-driven assembly process. By controlling the frictional interactions between the CNTs through atomic layer deposition, the densification degree of the CNT microstructure could be precisely controlled. Yao et al. (2021) significantly improved the interfacial wettability and interfacial strength between carbon fibers and a polycarbonate matrix by pre-coating the carbon fiber surface with polycarbonate nanoparticles. The densely packed microstructure formed by the polycarbonate nanoparticles on the fiber surface enhanced capillary action, facilitating resin infiltration into the interior of the carbon fiber bundles. As a result, the resin impregnation degree increased markedly to 93.48%, leading to improved interfacial adhesion. Overall, the interfacial shear strength of the composite was enhanced by 67.25%, while the tensile and flexural strengths increased by 41.06% and 22.16%, respectively. Caglar et al. (2019) addressed the issue of resin impregnation in fiber-

reinforced composite manufacturing by enhancing the capillary forces of glass fiber fabric through corona treatment. Capillary rise tests and permeability measurements confirmed a substantial enhancement in capillary force resulting from surface modification. Using ultraviolet light for rapid curing, they captured the flow front morphology and analyzed the interaction between capillary and viscous forces. This led to the optimization of the resin impregnation process, reducing pore formation and improving the molding quality of the composites.

The application of capillary pressure during the fabrication of composite microstructures leverages the capillarity of liquids within micro- or nanoscale pores, enabling the construction of high-performance architectures through the precise control of fluid flow and deposition. For instance, capillary action can be employed to align many randomly oriented short CNTs within a polymer matrix, thereby improving their dispersion and orientation. García et al. (2007) successfully fabricated composite microstructures by integrating commercially available thermosetting polymers with vertically aligned CNT forests using a capillary-force-driven wetting technique. The developed "immersion method" enabled polymer infiltration into the CNT forests via capillary action, achieving uniform wetting and preserving the vertical alignment of CNTs, even under challenging conditions such as high-viscosity and fast-curing epoxy resins. Shi et al. (2020) introduced a capillary-driven dynamic additive manufacturing method for 3D printing continuous carbon fiber reinforced thermoset composites, particularly addressing the challenges posed by high-viscosity and fast-curing epoxy resins. This method regulates the viscosity and curing degree of the liquid polymer using a localized thermal gradient, leveraging the capillary effect to guide the polymer into the gaps between carbon fibers where it is rapidly cured. This strategy allows for the *in-situ* curing of complex shapes.

5. Conclusions and perspectives

This review article systematically summarizes the mechanism and relevant applications of capillary theory in CFRP. Capillary action is defined as the spontaneous flow of liquid along a solid surface under the influence of surface tension at the liquid-air and liquid-solid interfaces, as well as the capillary pressure difference, without the application of external forces. The three fundamental equations are sequentially introduced: The capillary pressure theory, the average capillary pressure theory, and the interface enhancement theory. The infiltration behavior of liquids within fiber bundles is discussed in detail, along with the relevant theoretical models, experimental characterization methods for contact angles and capillary force testing, as well as numerical simulation techniques. The review concludes with a summary and outlook on future research on capillary effects in CFRP. The main suggestions are as follows:

1) The development of capillary force theoretical models should be combined with multiscale analysis. For short CNT fibers, scale effects become prominent at the nanoscale. Future research should focus on integrating multiscale simulation methods to better explain the mechanisms of capillary effects in complex porous structures and liquid infiltration processes.
2) The design of new materials should effectively leverage capillary pressure to achieve enhanced interfacial performance. Improving the interface properties between fibers and the matrix is key to enhancing the performance of CFRP.
3) Future studies should focus on understanding how capillary action influences interfacial performance, extending beyond mechanical properties to include thermal, electrical, and magnetic behaviors.

Acknowledgements

The authors acknowledge the financial support of the National Natural Science Foundation of China (Nos. 12202312 and 12472139), the Natural Science Foundation of Shanghai (No. 24ZR1471700), the Fundamental Research Funds for the Central Universities from Tongji University, and the Shanghai Gaofeng Project for University Academic Program Development.

Conflict of interest

The authors declare no competing interest.

References

Abry, J., Choi, Y., Chateauminois, A., et al. *In-situ* monitoring of damage in cfrp laminates by means of ac and dc measurements. Composites Science and Technology, 2001, 61(6): 855-864.

Ahn, K., Seferis, J., Berg, J. Simultaneous measurements of permeability and capillary pressure of thermosetting matrices in woven fabric reinforcements. Polymer Composites, 1991, 12(3): 146-152.

Amico, S., Lekakou, C. Axial impregnation of a fiber bundle. Part 2: Theoretical analysis. Polymer Composites, 2002, 23(2): 264-273.

Andriamananjara, K., Moulin, N., Bruchon, J., et al. Numerical modeling of local capillary effects in porous media as a pressure discontinuity acting on the interface of a transient bi-fluid flow. International Journal of Material Forming, 2019, 12(4): 675-691.

Armstrong, R. T., Sun, C., Mostaghimi, P., et al. Multiscale characterization of wettability in porous media. Transport in Porous Media, 2021, 140(1): 215-240.

Bayramli, E., Powell, R. The normal (transverse) impregnation of liquids into axially oriented fiber bundles. Journal of colloid and interface science, 1990, 138(2): 346-353.

Behera, A., Dupare, P., Thawre, M., et al. Effects of hygrothermal aging and fiber orientations on constant amplitude fatigue properties of cfrp multidirectional composite laminates. International Journal of Fatigue, 2020, 136: 105590.

Berry, J. D., Neeson, M. J., Dagastine, R. R., et al. Measurement of surface and interfacial tension using pendant drop tensiometry. Journal of Colloid and Interface Science, 2015, 454: 226-237.

Caglar, B., Tekin, C., Karasu, F., et al. Assessment of capillary phenomena in liquid composite molding. Composites Part A: Applied Science and Manufacturing, 2019, 120: 73-83.

Cai, J., Chen, Y., Liu, Y., et al. Capillary imbibition and flow of wetting liquid in irregular capillaries: A 100-year review. Advances in Colloid and Interface Science, 2022, 304: 102654.

Cai, J., Jin, T., Kou, J., et al. Lucas-washburn equation-based modeling of capillary-driven flow in porous systems. Langmuir, 2021, 37(5): 1623-1636.

Chang, C., Hourng, L., Wu, C. Numerical study on the capillary effect of resin transfer molding. Journal of Reinforced Plastics and Composites, 1997, 16(6): 566-586.

Chen, Y., Zhang, J., Li, Z., et al. Intelligent methods for optimization design of lightweight fiber-reinforced composite structures: A review and the-state-of-the-art. Frontiers in Materials, 2023a, 10: 1125328.

Chen, Y., Zhang, J., Li, Z., et al. Manufacturing technology of lightweight fiber-reinforced composite structures in aerospace: Current situation and toward intellectualization. Aerospace, 2023b, 10(3): 206.

Daniel, D., Vuckovac, M., Backholm, M., et al. Probing surface wetting across multiple force, length and time scales. Communications Physics, 2023, 6(1): 152.

Deng, Y., Chen, Y., Zhi, J., et al. Modeling capillary pressure in dual-scale fibrous structures for resin transfer molding processing of composites: A brief review and perspective. Capillarity, 2024, 13(3): 60-67.

Devalve, C., Pitchumani, R. Simulation of void formation in liquid composite molding processes. Composites Part A: Applied Science and Manufacturing, 2013, 51: 22-32.

Dresel, A., Teipel, U. Influence of the wetting behavior and surface energy on the dispersibility of multi-wall carbon nanotubes. Colloids and Surfaces A: Physicochemical and Engineering Aspects, 2016, 489: 57-66.

Duprat, C., Protière, S., Beebe, A. Y., et al. Wetting of flexible fibre arrays. Nature, 2012, 482(7386): 510-513.

García, E. J., Hart, A. J., Wardle, B. L., et al. Fabrication of composite microstructures by capillarity-driven wetting of aligned carbon nanotubes with polymers. Nanotechnology, 2007, 18(16): 165602.

Hong, X., Wang, P., Yang, W., et al. A multiscale bayesian method to quantify uncertainties in constitutive and microstructural parameters of 3D-printed composites. Journal of the Mechanics and Physics of Solids, 2024, 193: 105881.

Kim, H., Lim, J. H., Lee, K., et al. Direct measurement of contact angle change in capillary rise. Langmuir, 2020, 36(48): 14597-14606.

Lawrence, J. M., Neacsu, V., Advani, S. G. Modeling the impact of capillary pressure and air entrapment on fiber tow saturation during resin infusion in lcm. Composites Part A: Applied Science and Manufacturing, 2009, 40(8): 1053-1064.

Li, Z., Chen, Y., Wang, P., et al. A comprehensive multiscale model for elucidating strain-dependent piezoresistive behavior of porous mwcnts/polymer nanocomposites. International Journal of Solids and Structures, 2025, 320: 113516.

Li, X., Li, Z., Wang, S., et al. Electromechanically stable and flexible poro-hyperelastic composites for multimodal robotic tactile sensing. Composites Science and Technology, 2024, 257: 110821.

Li, Z., Wang, S., Ding, W., et al. Mechanically robust, flexible hybrid tactile sensor with microstructured sensitive composites for human-cyber-physical systems. Composites Science and Technology, 2023, 244: 110303.

Liu, M., Chen, Y., Cheng, W., et al. Controllable electromechanical stability of a torsional micromirror actuator with piezoelectric composite structure under capillary force. Capillarity, 2022, 5(3): 51-64.

Liu, P., Yang, R., Yu, A. Dynamics of wet particles in rotating drums: Effect of liquid surface tension. Physics of Fluids, 2011, 23(1): 013304.

Liu, P., Zhao, J., Li, Z., et al. Numerical simulation of multiphase multi-physics flow in underground reservoirs: Frontiers and challenges. Capillarity, 2024, 12(3): 72-79.

Michaud, V. Permeability properties of composite reinforcements, in Composite Reinforcements for Optimum Performance, edited by Michaud, V., Woodhead Publishing, Switzerland, pp. 443-472, 2021.

Neacsu, V., Obaid, A. A., Advani, S. G. Spontaneous radial capillary impregnation across a bank of aligned microcylinders e part I: Theory and model development. International Journal of Multiphase Flow, 2006, 32(6): 661-676.

Nordlund, M., Michaud, V. Dynamic saturation curve measurement for resin flow in glass fibre reinforcement. Composites Part A: Applied Science and Manufacturing, 2012, 43(3): 333-343.

Park, C. H., Lebel, A., Saouab, A., et al. Modeling and simulation of voids and saturation in liquid composite molding processes. Composites Part A: Applied Science and Manufacturing, 2011, 42(6): 658-668.

Pucci, M. F., Liotier, P. J., Drapier, S. Capillary wicking in a fibrous reinforcement-orthotropic issues to determine the capillary pressure components. Composites Part A: Applied Science and Manufacturing, 2015, 77: 133-141.

Schwartz, A. M. Capillarity – theory and practice. Industrial & Engineering Chemistry, 1969, 61(1): 10-21.

Shi, B., Shang, Y., Zhang, P., et al. Dynamic capillary-driven additive manufacturing of continuous carbon fiber composite. Matter, 2020, 2(6): 1594-1604.

Tawfick, S., Zhao, Z., Maschmann, M., et al. Mechanics of capillary forming of aligned carbon nanotube assemblies. Langmuir, 2013, 29(17): 5190-5198.

Teixidó, H., Staal, J., Caglar, B., et al. Capillary effects in fiber reinforced polymer composite processing: A review. Frontiers in Materials, 2022, 9: 809226.

Thomson, W. On the equilibrium of vapour at a curved surface

of liquid. Proceedings of the Royal Society of Edinburgh, 1872, 7: 63-68.

Uematsu, H., Horisawa, N., Horikida, T., et al. Effect of carbon fiber on the capillary extrusion behaviors of high-density polyethylene. Polymer Journal, 2013, 45(4): 449-456.

Wang, Y., Hahn, T. H. Afm characterization of the interfacial properties of carbon fiber reinforced polymer composites subjected to hygrothermal treatments. Composites Science and Technology, 2007, 67(1): 92-101.

Wang, C., Li, Y., Tong, L., et al. The role of grafting force and surface wettability in interfacial enhancement of carbon nanotube/carbon fiber hierarchical composites. Carbon, 2014, 69: 239-246.

Washburn, E. W. Note on a method of determining the distribution of pore sizes in a porous material. Proceedings of the National Academy of Sciences, 1921, 7(4): 115-116.

Yao, T., Zhang, X., Zhang, W., et al. Controlled attachment of polycarbonate nanoparticles on carbon fibers for increased resin impregnation and interfacial adhesion in carbon fiber composites. Composites Part B: Engineering, 2021, 224: 109218.

Yeager, M., Hwang, W. R., Advani, S. G. Prediction of capillary pressure for resin flow between fibers. Composites Science and Technology, 2016, 126: 130-138.

Young, T. An essay on the cohesion of fluids. Philosophical Transactions of the Royal Society of London, 1805, (95): 65-87.

Yuan, Y., Lee, T. Contact angle and wetting properties, in Surface Science Techniques, edited by G. Bracco and B. Holst, Springer Science & Business Media, Italy, pp. 3-34, 2013.

Zhang, L., Wang, J., Fuentes, C. A., et al. Wettability of carbon nanotube fibers. Carbon, 2017, 122: 128-140.

Zhang, J., Yang, W., Wang, P., et al. A pressure modulation approach to enhance mechanical properties of 3D-printed continuous fiber-reinforced composites. Composites Science and Technology, 2025, 270: 111277.

Zhang, Y., Zhang, J., Yang, W., et al. Chirality manipulation of 3d printed gyroidal scaffolds towards mechanical properties enhancement. Additive Manufacturing, 2024, 96: 104551.

Zhou, Y., Guan, W., Zhao, C., et al. Spontaneous imbibition behavior in porous media with various hydraulic fracture propagations: A pore-scale perspective. Advances in Geo-Energy Research, 2023, 9(3): 185-197.

Zhou, Y., Guan, W., Zhao, C., et al. Numerical methods to simulate spontaneous imbibition in microscopic pore structures: A review. Capillarity, 2024, 11(1): 1-21.